Proc. R. Soc. Lond. A **424**, 279–288 (1989)
Printed in Great Britain

Fringes decorating anticaustics in ergodic wavefunctions

BY M. V. BERRY, F.R.S.
H. H. Wills Physics Laboratory, Tyndall Avenue, Bristol BS8 1TL, U.K.

(*Received* 13 *February* 1989)

The probability density Π is calculated for quantum eigenstates near spatial boundaries of classically chaotic regions. By contrast with integrable systems, for which the classical Π diverges on classical boundaries, which are caustics, in chaotic systems the classical Π does not diverge but vanishes abruptly in a way that depends on the number of freedoms N; the boundaries are anticaustics. Quantum mechanics softens anticaustics, to give Π in terms of a set of canonical diffraction patterns, one for each N; these are studied in detail. The appropriate definition of Π involves averaging over eigenstates in an energy range larger than $O(h)$ but smaller than $O(h^{\frac{2}{3}})$ (where h is Planck's constant), that is over a range of $\Delta\mathcal{N}$ states near the $\mathcal{N}$th, where $\mathcal{N}^{1-1/N} \ll \Delta\mathcal{N} \ll \mathcal{N}^{1-2/3N}$.

1. INTRODUCTION

According to the simplest semiclassical theory, the spatial probability density $|\psi_n(\boldsymbol{r})|^2$ of quantum eigenstates ψ_n with energy E_n near E is proportional to the density of the projection of a typical classical orbit from phase space $\boldsymbol{x} = (\boldsymbol{r}, \boldsymbol{p})$ 'down' momentum $\boldsymbol{p}$ onto configuration space (Berry 1977*a*; Voros 1979; reviewed by Berry (1983) and Ozorio de Almeida (1988)). If the classical system is integrable, a typical orbit sweeps out a torus, whose projection is singular at its boundary which is a caustic of the orbit. Then in the classical limit $|\psi_n|^2$ diverges at the boundary in the same way (inverse square root) whatever the number of freedoms N.

Here I will concentrate on the opposite situation, where the system is ergodic and therefore non-integrable (if $N \geqslant 2$). Then a typical orbit explores the whole energy surface, and the simple theory gives

$$|\psi_n(\boldsymbol{r})|^2 \propto \int \mathrm{d}^N \boldsymbol{p} \delta\{E - H(\boldsymbol{x})\} \quad \boldsymbol{x} \equiv (\boldsymbol{r}, \boldsymbol{p}), \tag{1}$$

where $H(\boldsymbol{x})$ is the hamiltonian. As $\boldsymbol{r}$ crosses the boundary of the classically allowed region at energy E, this predicts (Berry 1977*a*) that the probability density does not diverge, but vanishes abruptly in a manner that depends on N: if $N = 2$ the density has a step discontinuity and if $N > 2$ it vanishes as $(-\xi)^{(\frac{1}{2}N-1)}$, where ξ is a coordinate increasing across the boundary. Because of this non-divergence the boundary is called an anticaustic. (In the trivial case $N = 1$, the system is integrable as well as ergodic, and the projected density (1) diverges because the classical boundary is a caustic.)

My aim is to improve on the crude approximation (1) and thereby obtain a more

refined description of quantum wavefunctions near anticaustics. The result will be that the singularities are smoothed and decorated by oscillations whose form depends only on N (apart from scaling).

We cannot build a theory for individual eigenstates, because these are often dominated by interference effects of a different sort, associated with classical closed orbits. These effects were observed in numerical computations and examined theoretically by Heller (1984, 1986), who called them 'scars', and also studied analytically by Bogomolny (1988) and by Berry (1989) (hereafter called I). The effects of the scars can, however, be eliminated by averaging the probability densities of a group of states in an energy range, centred on E, of width $\epsilon > h/T$ where T is the period of the shortest closed orbit and h is Planck's constant. Later we shall see that such averaging need not destroy the coherence of the anticaustic fringes we are interested in.

Therefore we study the *smoothed spectral probability density*

$$\Pi(\boldsymbol{r};E,\epsilon) \equiv \sum_n |\psi_n(\boldsymbol{r})|^2 \delta_\epsilon(E-E_n), \tag{2}$$

where δ_ϵ denotes the smoothed delta function

$$\delta_\epsilon(x) \equiv -(1/\pi)\,\mathrm{Im}\,1/(x+\mathrm{i}\epsilon). \tag{3}$$

In terms of the hamiltonian operator $\hat{H}$,

$$\Pi(\boldsymbol{r};E,\epsilon) = \langle \boldsymbol{r}|\delta_\epsilon(E-\hat{H})|\boldsymbol{r}\rangle. \tag{4}$$

We will calculate Π as the projection of the spectral Wigner function, (see I) that is as

$$\Pi(\boldsymbol{r};E,\epsilon) = \frac{1}{h^N}\int \mathrm{d}^N\boldsymbol{p}\,W(\boldsymbol{x};E,\epsilon), \tag{5}$$

where

$$W(\boldsymbol{r};E,\epsilon) = h^N\,\mathrm{Tr}\,\delta_\epsilon(E-\hat{H})\,\delta(\hat{\boldsymbol{x}}-\boldsymbol{x}) \tag{6}$$

(the delta function involving the phase space operators $\hat{\boldsymbol{r}},\hat{\boldsymbol{p}}$ is defined by its Fourier transform). The simplest semiclassical approximation, which gives (1), is obtained by neglecting all commutators and evaluating the trace as an integral over phase space:

$$W(\boldsymbol{x};E,\epsilon) \approx \delta_\epsilon\{E-H(\boldsymbol{x})\}. \tag{7}$$

The most convenient entry point for a semiclassical theory enabling us to improve on this lowest-order result is a representation of W as the time Fourier transform of the Wigner propagator, that is as

$$W(\boldsymbol{x};E,\epsilon) = \frac{2}{h}\,\mathrm{Re}\int_0^\infty \mathrm{d}t\,K_\mathrm{W}(\boldsymbol{x},t)\exp\{\mathrm{i}(E+\mathrm{i}\epsilon)\,t/\hbar\}, \tag{8}$$

where

$$K_\mathrm{W}(x,t) \equiv h^N\,\mathrm{Tr}\exp(-\mathrm{i}\hat{H}t/\hbar)\,\delta(\hat{\boldsymbol{x}}-\boldsymbol{x}). \tag{9}$$

Our ϵ smoothing damps out the effects of long classical orbits, so we need a semiclassical approximation to K_W only for short times.

2. Smoothed spectral Wigner function

In I I showed that the general semiclassical approximation for the Wigner propagator (9) can be written

$$K_{\mathrm{W}}(\boldsymbol{x},t) \approx 2^N \sum_j \exp\left\{-\mathrm{i}\int_0^t \mathrm{d}t' H(\boldsymbol{x}_j^*(\boldsymbol{x},t'))/\hbar + \gamma_j\right\} \Big/ [\det\{m_j + I\}]^{\frac{1}{2}}. \tag{10}$$

In this formula, j labels the contributing classical paths: those which in time t connect points A and B whose midpoint is $\boldsymbol{x}$ (figure 1); $\boldsymbol{x}^*$ is any point on the path, γ is a phase, and m the $2N \times 2N$ matrix relating small displacements at A and B.

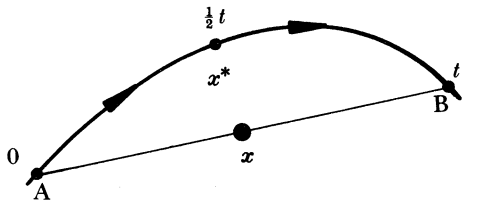

Figure 1. Classical path contributing to Wigner propagator at $\boldsymbol{x}, t$.

As $t \to 0$, only one classical path contributes: almost straight and linking phase points A and B that are close together. Then γ is zero and m close to the unit matrix. We need the energy of this path. To lowest order the energy is simply $H(\boldsymbol{x})$, but this just reproduces the result (7) that we seek to improve. To capture the oscillations of W we must find the next correction to the energy.

We proceed by adapting a method from I. Referring to figure 1, choose $\boldsymbol{x}^*$ to be the point reached at time $\frac{1}{2}t$ along the orbit from A to B. Expanding to second order about $\frac{1}{2}t$ gives the endpoints as

$$\left.\begin{aligned} \boldsymbol{x}_{\mathrm{B}} &= \boldsymbol{x}^* + \tfrac{1}{2}t\,\dot{\boldsymbol{x}}_{\frac{1}{2}} + \tfrac{1}{8}t^2\,\ddot{\boldsymbol{x}}_{\frac{1}{2}} + \ldots, \\ \boldsymbol{x}_{\mathrm{A}} &= \boldsymbol{x}^* - \tfrac{1}{2}t\,\dot{\boldsymbol{x}}_{\frac{1}{2}} + \tfrac{1}{8}t^2\,\ddot{\boldsymbol{x}}_{\frac{1}{2}} + \ldots, \end{aligned}\right\} \tag{11}$$

where dots denote time derivatives on the orbit. Taking the midpoint of A and B gives $\boldsymbol{x}^*$, also to second order, as

$$\boldsymbol{x}^* = \boldsymbol{x} - \tfrac{1}{8}t^2\,\ddot{\boldsymbol{x}} + \ldots. \tag{12}$$

The energy of the path is thus

$$\left.\begin{aligned} H(\boldsymbol{x}^*) &= H(\boldsymbol{x}) - \tfrac{1}{8}t^2\,\ddot{\boldsymbol{x}}\cdot\nabla_x H(\boldsymbol{x}) + \ldots \\ &= H(\boldsymbol{x}) + \tfrac{1}{8}t^2\,\dot{\boldsymbol{x}} \wedge \ddot{\boldsymbol{x}} + \ldots, \end{aligned}\right\} \tag{13}$$

where the second equality is obtained from Hamilton's equations and the definition

$$\dot{\boldsymbol{x}} \wedge \ddot{\boldsymbol{x}} \equiv -\dot{\boldsymbol{q}}\cdot\ddot{\boldsymbol{p}} + \dot{\boldsymbol{p}}\cdot\ddot{\boldsymbol{q}}. \tag{14}$$

Substituting into (10) now gives the short-time Wigner propagator as

$$K_{\mathrm{W}} \approx \exp\{-\mathrm{i}[H(\boldsymbol{x})\,t + \tfrac{1}{24}t^3\,\dot{\boldsymbol{x}} \wedge \ddot{\boldsymbol{x}}]/\hbar\}. \tag{15}$$

To get the spectral Wigner function we must perform the time integral (8). This involves the smoothing energy ϵ. We will ignore this dependence on ϵ, for a reason to be explained presently. The integral can be expressed in terms of the Airy function (Abramowitz & Stegun 1964):

$$W(\boldsymbol{x};E,\epsilon) \approx \frac{2}{(\hbar^2|\dot{\boldsymbol{x}}\wedge\ddot{\boldsymbol{x}}|)^{\frac{1}{3}}}\,\mathrm{Ai}\left\{\frac{2[H(\boldsymbol{x})-E]}{(\hbar^2\dot{\boldsymbol{x}}\wedge\ddot{\boldsymbol{x}})^{\frac{1}{3}}}\right\}. \tag{16}$$

This describes fringes decorating the energy surface $H = E$. The fringes close to the energy surface have separation of order $\hbar^{\frac{2}{3}}$. Their coherence will be maintained in spite of the energy smoothing if ϵ is not too large. However, ϵ must not be too small if it is to perform the function for which we introduced it, namely damping out the contributions of the closed orbits. We achieve both these aims if we choose ϵ in the range

$$h/T \ll \epsilon \ll (\hbar^2|\dot{\boldsymbol{x}}\wedge\ddot{\boldsymbol{x}}|)^{\frac{1}{3}} \tag{17}$$

and this is the range for which (16) is valid. Note that in the asymptotic limit $h\to 0$ the scales h and $\hbar^{\frac{2}{3}}$ separate and the inequalities (17) become less restrictive.

Airy oscillations in Wigner functions are familiar in the context of integrable systems (Balazs & Zipfel 1973; Berry 1977*b*; Balazs 1980). The result (16) shows that they also occur in multidimensional ergodic systems.

3. Projection onto configuration space

The anticaustic fringes we seek to describe are obtained from the projection (5) of the Airy fringes (16). There is no essential loss of generality, and the formulae are more transparent, if we carry out the calculations for the familiar case of a non-relativistic particle in a scalar potential:

$$H(\boldsymbol{x}) = \tfrac{1}{2}|\boldsymbol{p}|^2/m + V(\boldsymbol{r}). \tag{18}$$

The classical boundary is defined by $\boldsymbol{p} = 0$, that is $V(\boldsymbol{r}) = E$. From Hamilton's equations we easily find

$$\dot{\boldsymbol{x}}\wedge\ddot{\boldsymbol{x}} = |\nabla V(\boldsymbol{r})|^2/m + (\boldsymbol{p}\cdot\nabla)^2 V(\boldsymbol{r})/m^2. \tag{19}$$

For $\boldsymbol{r}$ near the anticaustic, the concentration of the spectral Wigner function (16) near the energy surface implies that only small $\boldsymbol{p}$ contribute to the projection integral (5). Therefore, we can neglect the second term in (19) and because W now depends only on the length p of $\boldsymbol{p}$ we can evaluate (5) in spherical coordinates. Introducing the area of the N-dimensional unit sphere,

$$\omega_N = \frac{2\pi^{\frac{1}{2}N}}{\Gamma(\frac{1}{2}N)}, \tag{20}$$

we obtain the spectral probability density

$$\Pi(\boldsymbol{r};E,\epsilon) \approx \frac{2\omega_N}{h^N(|\hbar\nabla V|^2/m)^{\frac{1}{3}}}\int_0^\infty \mathrm{d}p\, p^{N-1}\,\mathrm{Ai}\left\{\frac{2(\frac{1}{2}p^2/m+V-E)}{(|\hbar\nabla V|^2/m)^{\frac{1}{3}}}\right\}. \tag{21}$$

This involves the natural variable

$$X \equiv \frac{2[V(\boldsymbol{r})-E]}{(|\hbar\nabla V(\boldsymbol{r})|^2/m)^{\frac{1}{3}}} \approx 2\left(\frac{m|\nabla V|}{\hbar^2}\right)^{\frac{1}{3}}\xi, \tag{22}$$

where ξ is a coordinate normal to the anticaustic and reckoned negative in the allowed region $E > V$, and where in the last expression ∇V is evaluated on the classical boundary.

Thus

$$\Pi(\boldsymbol{r};E,\epsilon) \approx 2(m/h^2)^{\frac{1}{2}N}(|\hbar\nabla V|^2/m)^{\frac{1}{3}(\frac{1}{2}N-1)}A_N(X), \tag{23}$$

where $A_N(X)$ is the *canonical anticaustic fringe pattern* for N freedoms, defined by

$$A_N(X) \equiv \omega_N \int_0^\infty \mathrm{d}P\,P^{N-1}\,\mathrm{Ai}\,(P^2+X). \tag{24}$$

These two equations constitute the main result of this paper.

4. Anticaustic fringe patterns

Because Π is a density, the canonical integrals $A_N(X)$ must be positive. For $N = 1$ this follows from the known relation

$$A_1(X) = 2^{\frac{2}{3}}\pi\,\mathrm{Ai}^2\,(X/2^{\frac{2}{3}}). \tag{25}$$

Positivity for $N > 1$ is confirmed by the following representation, derived from (24) in Appendix A:

$$A_N(X) = 2^{\frac{2}{3}}\pi\omega_{N-1}\int_0^\infty \mathrm{d}P\,P^{N-2}\,\mathrm{Ai}^2\left(\frac{P^2+X}{2^{\frac{2}{3}}}\right). \tag{26}$$

(For integrable systems, Berry & Wright (1980) found a different generalization of (25), in the form of infinitely many 'projection identities' corresponding to diffraction catastrophes associated with more complicated caustics.)

In understanding the fringe patterns, it helps to know their asymptotic forms as $X \to \pm\infty$ and their values at $X = 0$. As shown in Appendix B, these are as follows:

$$A_N(X) \underset{X\to-\infty}{\to} \frac{\pi^{\frac{1}{2}N}}{\Gamma(\frac{1}{2}N)}|X|^{\frac{1}{2}N-1} + \frac{\pi^{\frac{1}{2}(N-1)}}{|X|^{\frac{1}{4}(N+1)}}\sin\{\tfrac{2}{3}|X|^{\frac{3}{2}} - \tfrac{1}{4}(N-1)\,\pi\}, \tag{27a}$$

$$\underset{X=0}{\to} \frac{\pi^{\frac{1}{2}N}}{3^{\frac{1}{6}(4+N)}\,\Gamma\{\frac{1}{6}(4+N)\}}, \tag{27b}$$

$$\underset{X\to+\infty}{\to} \frac{\pi^{\frac{1}{2}(N-1)}}{2X^{\frac{1}{4}(N+1)}}\exp\{-\tfrac{2}{3}X^{\frac{3}{2}}\}. \tag{27c}$$

The first term for $X \to -\infty$ corresponds to the simple theory based on (1). It follows from (22) that the oscillations for $X \to -\infty$ have precisely the de Broglie wavelength h/p, where p is the length of the classical momentum at a distance ξ from the anticaustic. The decay for $X \to +\infty$ describes tunnelling into the

classically forbidden region beyond the anticaustic (see also Wilkinson & Hannay 1987).

Figure 2 shows the canonical anticaustic patterns for $N = 2$ and $N = 3$, as well as the ordinary caustic intensity pattern for $N = 1$ (originally derived by Airy (1838)). The accuracy of the asymptotics (27) for large $|X|$ is obvious.

When N is odd, the integrals A_N can be evaluated in a finite series, giving the following formula (Appendix C) in terms of Airy functions and their derivatives (denoted by numbers in square brackets):

$$A_N(X) \underset{(N\text{odd})}{=} \frac{\omega_N \pi}{2^{\frac{1}{3}(2N-1)}} \sum_{k=0}^{N-1} \frac{(N-1)!(-1)^{\frac{1}{2}(N-1)+k}}{k!(N-1-k)!} \mathrm{Ai}^{[k]}(X/2^{\frac{2}{3}})\,\mathrm{Ai}^{[N-1-k]}(X/2^{\frac{2}{3}}). \quad (28)$$

For $N = 1$ this reproduces (25); for $N = 3$ it gives

$$A_3(X) = 2^{\frac{4}{3}}\pi^2\{(\mathrm{Ai}^{[1]}(X/2^{\frac{2}{3}}))^2 - (X/2^{\frac{2}{3}})(\mathrm{Ai}\,(X/2^{\frac{2}{3}}))^2\}. \quad (29)$$

5. Discussion

I have shown that anticaustic singularities at the boundaries of classically allowed regions in space are softened by quantum mechanics in a characteristic way, embodied in the formulae (23) and (24). If, as I hope, this work stimulates experiments (numerical or otherwise) to test its predictions, it should be understood that the canonical diffraction patterns emerge clearly only after averaging the probability densities of a group of eigenstates in an energy range ϵ satisfying (17). These inequalities ensure that ϵ is large enough to damp out the confusing effects of scars of classical closed orbits, but not so large as to smooth away the anticaustic fringes.

In exploratory computations it is often convenient to work with scaling potentials, satisfying

$$V(\alpha \boldsymbol{r}) = \alpha^{\mu} V(\boldsymbol{r}). \quad (30)$$

Then the inequalities for ϵ can be expressed as inequalities for the number of states $\Delta\mathcal{N}$ that must be averaged to see the anticaustic fringes for states near the $\mathcal{N}$th. We obtain

$$\alpha_{\mu}\mathcal{N}^{1-1/N} \ll \Delta\mathcal{N} \ll \beta_{\mu}\mathcal{N}^{1-2/3N}, \quad (31)$$

where α_{μ} and β_{μ} are constants. As $\mathcal{N}$ increases, the upper and lower bounds separate, their ratio being $\mathcal{N}^{1/3N}$, which must be large for the fringes to be observable. This condition is more restrictive for more freedoms. At present the only realistic prospect of a test is for $N = 2$, and would require (at least) averaging over several tens of states near the 1000th.

It is important that the averaging is over energy, that is over a group of eigenstates. This is not equivalent to averaging over a region of space for an individual state. Spatial averaging would fail to eliminate the scars because their fringe spacing (transverse to the closed orbit) is $O(\hbar^{\frac{1}{2}})$ (Bogomolny 1988; Berry 1989) which is larger than the spacing $O(\hbar^{\frac{2}{3}})$ near the anticaustics. Energy averaging is successful because it eliminates the scar fringes by damping their amplitude (proportional to $\exp(-\epsilon T/\hbar$ for orbit with period T).

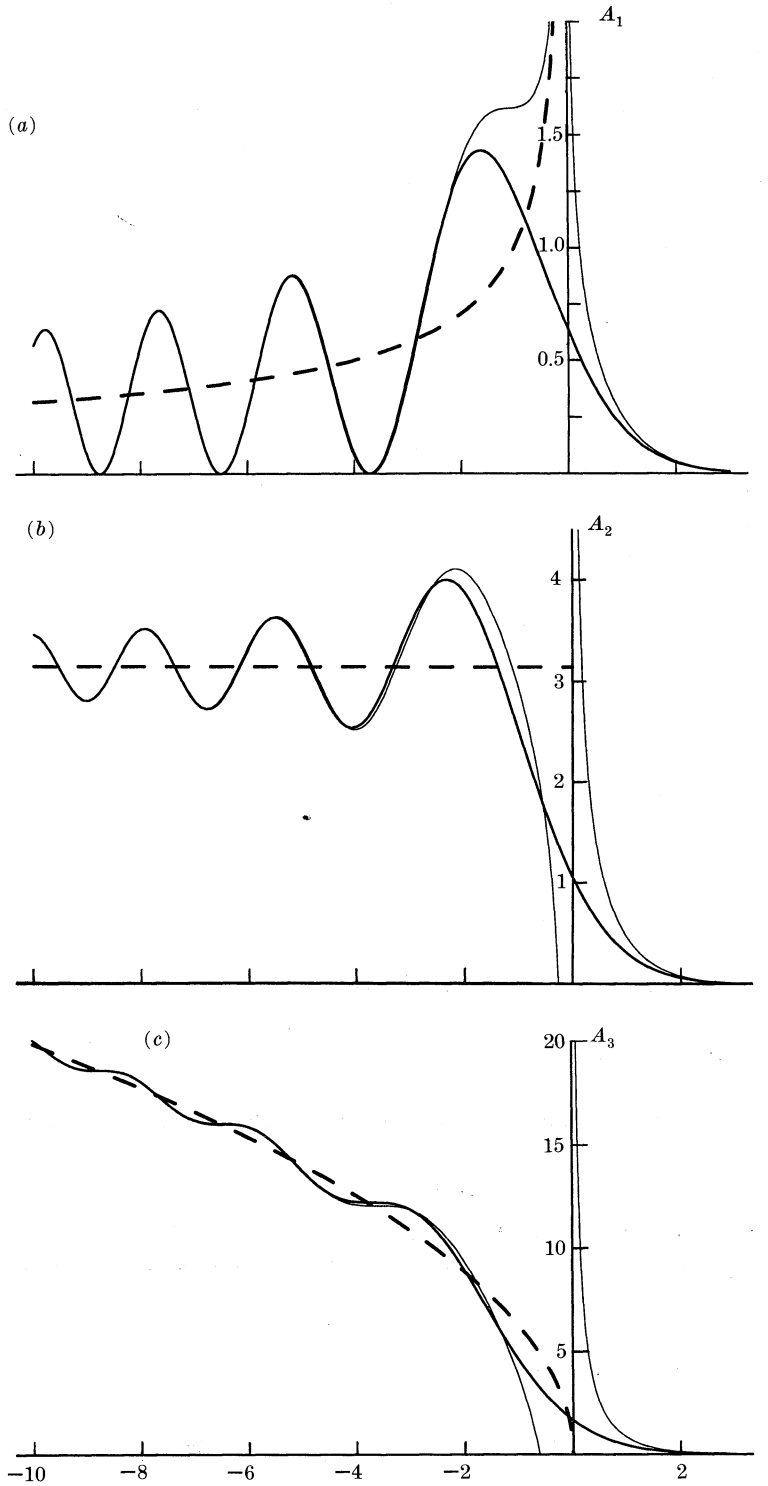

FIGURE 2. Anticaustic diffraction patterns, for (*a*) $N = 1$; (*b*) $N = 2$; (*c*) $N = 3$. Heavy lines: canonical integrals $A_N(X)$ defined by (24); light lines: asymptotic approximation (27*a*) and (27*c*); dashed lines: simplest semiclassical theory based on (1).

The theory given here is the simplest that yields the anticaustic fringes. Several refinements are possible. For example, the effect of ϵ could be made more explicit by Lorentz averaging Π in (23) or W in (16); however any ϵ large enough for this to make an appreciable difference would violate (17) and so smooth away the fringes. Or the t expansion (13) could be replaced by a geometric construction based directly on (10), to yield a uniform approximation whose validity extends deep into the allowed region, far from the anticaustic. This would be analogous to uniform expansions for integrable systems (Berry 1977*b*; Ozorio de Almeida 1988), but would be less interesting in the ergodic case because fringes deep in the allowed region have spacing $O(h)$ and so are eliminated by the ϵ averaging.

I thank Professor A. M. Ozorio de Almeida for helpful conversations.

Appendix A

This is the derivation of the positivity relation (26). Writing the integral (24) in terms of the N cartesian (rather than polar) coordinates of $\boldsymbol{P}$, and using the integral representation of Ai, we have

$$A_N(X) = \frac{1}{2\pi}\int_{-\infty}^{\infty} \mathrm{d}t \int_{-\infty}^{\infty} \mathrm{d}P_N \int_{-\infty}^{\infty} \mathrm{d}P_1 \ldots \int_{-\infty}^{\infty} \mathrm{d}P_{N-1} \exp\{\mathrm{i}\Phi\}, \tag{A 1}$$

where

$$\Phi = \tfrac{1}{3}t^3 + (X + P_N^2)t + \sum_{i=1}^{N-1} P_i^2 t. \tag{A 2}$$

In terms of new variables,

$$t \equiv u + v; \quad P_N \equiv u - v, \tag{A 3}$$

Φ becomes

$$\Phi = \tfrac{4}{3}u^3 + \left(X + \sum_{i=1}^{N-1} P_i^2\right)u + \tfrac{4}{3}v^3 + \left(X + \sum_{i=1}^{N-1} P_i^2\right)v. \tag{A 4}$$

The u and v integrals separate and each gives an Airy function, so

$$A_N(X) = 2^{\frac{2}{3}}\pi \int_{-\infty}^{\infty} \mathrm{d}P_1 \ldots \int_{-\infty}^{\infty} \mathrm{d}P_N \,\mathrm{Ai}^2\left\{\left(X + \sum_{i=1}^{N-1} P_i^2\right)\Big/ 2^{\frac{2}{3}}\right\}. \tag{A 5}$$

Equation (26) is now obtained by replacing the Ps with polar coordinates in $N-1$ dimensions.

Appendix B

This is the derivation of the limiting forms (27). As $X \to -\infty$ the integral (24) is dominated by the region near $P = \sqrt{|X|}$ where the Airy function is large. Therefore we write

$$P \equiv \sqrt{|X|} + u \tag{B 1}$$

and expand to lowest order in u:

$$A_N(X) \approx \omega_N |X|^{\frac{1}{2}(N-1)} \int_{-\infty}^{\infty} \mathrm{d}u \,\mathrm{Ai}\,(2u\sqrt{|X|}) = \tfrac{1}{2}\omega_N |X|^{\frac{1}{2}N-1}, \tag{B 2}$$

which is the first term in (27*a*).

In addition, there is an oscillatory contribution from the endpoint $P = 0$. Near $P = 0$ the Airy function can be replaced by its asymptotic form for large negative argument, giving

$$\begin{aligned} A_N^{\mathrm{osc}}(X) &\approx \frac{2\pi^{\frac{1}{2}(N-1)}}{\Gamma(\frac{1}{2}N)|X|^{\frac{1}{4}}}\int_0^\infty \mathrm{d}P\,P^{N-1}\sin\{\tfrac{2}{3}(|X|-P^2)^{\frac{3}{2}}+\tfrac{1}{4}\pi\} \\ &\approx \frac{2\pi^{\frac{1}{2}(N-1)}}{\Gamma(\frac{1}{2}N)|X|^{\frac{1}{4}}}\mathrm{Im}\int_0^\infty \mathrm{d}P\,P^{N-1}\exp\{\mathrm{i}[\tfrac{2}{3}|X|^{\frac{3}{2}}-P^2|X|^{\frac{1}{2}}+\tfrac{1}{4}\pi]\} \\ &= \frac{\pi^{\frac{1}{2}(N-1)}}{\Gamma(\frac{1}{2}N)|X|^{\frac{1}{4}(N+1)}}\mathrm{Im}\exp(\tfrac{2}{3}\mathrm{i}|X|^{\frac{3}{2}}+\tfrac{1}{4}\mathrm{i}\pi)\int_0^\infty \mathrm{d}u\,u^{\frac{1}{2}N-1}\exp(-\mathrm{i}u). \end{aligned} \tag{B 3}$$

The second term in (27*a*) follows on deforming the contour and evaluating the integral as a gamma function.

As $X \to +\infty$ the maximum of the Airy function lies outside the range of integration, so the dominant contribution comes from the endpoint, near which Ai can be replaced by its asymptotic form for large positive argument, giving

$$\begin{aligned} A_N(X) &\approx \frac{\pi^{\frac{1}{2}(N-1)}}{\Gamma(\frac{1}{2}N)X^{\frac{1}{4}}}\int_0^\infty \mathrm{d}P\,P^{N-1}\exp\{-\tfrac{2}{3}(X+P^2)^{\frac{3}{2}}\} \\ &\approx \frac{\pi^{\frac{1}{2}(N-1)}}{\Gamma(\frac{1}{2}N)X^{\frac{1}{4}}}\int_0^\infty \mathrm{d}P\,P^{N-1}\exp\{-\tfrac{2}{3}X^{\frac{3}{2}}-P^2X^{\frac{1}{2}}\}. \end{aligned} \tag{B 4}$$

The formula (27*c*) follows after replacing the integration variable by $u \equiv P\sqrt{X}$.

When $X = 0$ we employ the integral representation for the Airy function:

$$\begin{aligned} A_N(0) &= \frac{\omega_N}{2\pi}\int_{-\infty}^\infty \mathrm{d}t\int_0^\infty \mathrm{d}P\,P^{N-1}\exp\{\mathrm{i}[\tfrac{1}{3}t^3+P^2t]\} \\ &= \frac{\omega_N}{4\pi}\int_{-\infty}^\infty \mathrm{d}t\,\frac{\exp\{\mathrm{i}(\frac{1}{3}t^3+\frac{1}{4}N\pi\,\mathrm{sgn}\,(t))\}}{|t|^{\frac{1}{2}N}}\int_0^\infty \mathrm{d}u\,u^{\frac{1}{2}N-1}\exp(-u) \\ &= \pi^{\frac{1}{2}N-1}\,\mathrm{Re}\int_0^\infty \mathrm{d}t\,\frac{\exp\{\mathrm{i}(\frac{1}{3}t^3+\frac{1}{4}N\pi)\}}{|t|^{\frac{1}{2}N}} \\ &= \frac{\pi^{\frac{1}{2}N-1}}{3^{\frac{1}{6}(N+4)}}\cos\{\tfrac{1}{6}\pi(N+1)\}\,\Gamma(\tfrac{1}{3}-\tfrac{1}{6}N). \end{aligned} \tag{B 5}$$

The formula (27*b*) now follows from the reflection formula for $\Gamma(x)$. (This derivation is valid for N such that the t integrals converge, but by analytic continuation the result holds for all N.)

Appendix C

This is the derivation of the formula (28) for N odd. Starting with (24) we replace Ai by its integral representation and use the transformation (A 3) with P replacing P_N. Because $N-1$ is even we can extend the range of the P integration to the whole real axis, giving

$$A_N(X) = \frac{\omega_N}{4\pi}\int_{-\infty}^{\infty} \mathrm{d}P\, P^{N-1} \int_{-\infty}^{\infty} \mathrm{d}t \exp\{\mathrm{i}[\tfrac{1}{3}t^3 + (P^2+X)\,t]\}$$

$$= \frac{\omega_N}{2\pi}\int_{-\infty}^{\infty} \mathrm{d}u \int_{-\infty}^{\infty} \mathrm{d}v (u-v)^{N-1} \exp\{\mathrm{i}(\tfrac{4}{3}u^3 + uX + \tfrac{4}{3}v^3 + vX)\}. \qquad \text{(C 1)}$$

Binomial expansion of $(u-v)^{N-1}$ enables the u and v integrals to be evaluated separately by using

$$\int_{-\infty}^{\infty} \mathrm{d}u\, u^k \exp\{\mathrm{i}[\tfrac{4}{3}u^3 + uX]\} = \frac{(-\mathrm{i})^k \pi}{2^{\frac{2}{3}(k+1)}} \mathrm{Ai}^{[k]}\{X/2^{\frac{2}{3}}\}. \qquad \text{(C 2)}$$

The formula (28) now follows immediately.

References

Abramowitz, M. & Stegun, I. A. 1964 *Handbook of mathematical functions.* Washington, D.C.: National Bureau of Standards.

Airy, G. B. 1838 *Trans. Camb. phil. Soc.* **6**, 379–403.

Balazs, N. L. 1980 *Physica* A **102**, 236–254.

Balazs, N. L. & Zipfel, G. G. Jr 1973 *Ann. Phys., New York* **77**, 139–156.

Berry, M. V. 1977*a* *J. Phys.* A **10**, 2083–2091.

Berry, M. V. 1977*b* *Phil. Trans. R. Soc. Lond.* A **287**, 237–271.

Berry, M. V. 1983 In *Chaotic behavior of deterministic systems*, Les Houches Lectures XXXVI (ed. G. Iooss, R. H. G. Helleman & R. Stora), pp. 171–271. Amsterdam: North-Holland.

Berry, M. V. 1989 *Proc. R. Soc. Lond.* A **423**, 219–231.

Berry M. V. & Wright, F. J. 1980 *J. Phys.* A **13**, 149–160.

Bogomolny, E. B. 1988 *Physica* D **31**, 169–189.

Heller, E. J. 1984 *Phys. Rev. Lett.* **53**, 1515–1518.

Heller, E. J. 1986 In *Quantum chaos and statistical nuclear physics* (ed. T.-H. Seligman & H. Nishioka), (Springer Lecture Notes in Physics, no. 93), pp. 162–181.

Ozorio de Almeida, A. M. 1988 *Hamiltonian systems: chaos and quantization.* Cambridge University Press.

Voros, A. 1979 In *Stochastic behaviour in classical and quantum hamiltonian systems* (ed. G. Casati & J. Ford), pp. 326–333. Springer Lecture Notes in Physics, no. 93.

Wilkinson, M. & Hannay, J. H. 1987 *Physica* D **27**, 201–212.